Duality and Sheared Analytic Response in Mechanism-Based Metamaterials

Michael Czajkowski and D. Zeb Rocklin
School of Physics, Georgia Institute of Technology, Atlanta, Georgia 30332, USA

(Received 7 July 2022; revised 17 November 2023; accepted 28 November 2023; published 8 February 2024)

Mechanical metamaterials designed around a zero-energy pathway of deformation known as a mechanism, challenge the conventional picture of elasticity and generate complex spatial response that remains largely uncharted. Here, we present a unified theoretical framework to showing that the presence of a unimode in a 2D structure generates a space of anomalous zero-energy *sheared analytic modes*. The spatial profiles of these stress-free strain patterns is dual to equilibrium stress configurations. We show a transition at an exceptional point between bulk modes in structures with conventional Poisson ratios (anauxetic) and evanescent surface modes for negative Poisson ratios (auxetic). We suggest a first application of these unusual response properties as a switchable signal amplifier and filter for use in mechanical circuitry and computation.

DOI: 10.1103/PhysRevLett.132.068201

Classical elasticity is a field theory describing a structure's deformation from a single zero-energy shape. In contrast, a growing number of strategies and methods to program special energy-free pathways of deformation directly into designer materials [1–6] generate structures with continuous manifolds of (nearly) zero-energy shapes. Such pathways, known as mechanisms, fundamentally challenge the classical picture of elasticity by setting common elastic constants to anomalous zero or negative values [1,2,7–16]. Even further beyond conventional elasticity, structures have been developed with "odd" elastic constants [17], multistability [18], geometric frustration [19,20], and hierarchical elasticity [21–23], and yet the generic consequences of a single mechanism on elastic response have still remained largely unexplored.

A recent series of investigations has revealed that a purely dilational mechanism fundamentally changes the response of a continuum material by introducing an associated space of conformal soft modes [24–27]. In the continuum limit of a perfect mechanism, these modes cost zero energy, and it was suggested that such a nontrivial soft mode space would come paired with any generic mechanism even outside the dilational limit [14,25–28], and some indicative nonlinear examples of this phenomenon have since been identified [26,27]. Further, the introduction of such a class of stress-free deformations into the force-balanced deformations has unknown implications for the profiles of stress that are supported. Therefore, the question presses: how is the overall space of supported deformations necessarily changed by mechanism design?

Here, rather than focus on a particular microstructure or type of mechanism, we explore how the presence of an arbitrary mechanism necessarily determines a two-dimensional structure's non-uniform equilibrium response, in much the same way that conventional translational and rotational symmetries necessarily give rise to elastic waves as Goldstone bosons [29]. We find that the impact of an arbitrary mechanism is to generate spatial patterns of stress-free strains that are dual to the system's permitted stresses. Both are analytic in a particular set of sheared coordinates, which we introduce here, and we show that the spatial character of these deformation patterns is controlled by an exceptional point in the Poisson's ratio ν at $\nu = 0$.

Elasticity theory for generic planar mechanism metamaterials.—Consider an elastic solid undergoing a deformation such that matter initially located at material coordinates $\mathbf{R} = (x, y)$ is displaced by $\mathbf{u}(\mathbf{R})$. Because the system is translationally invariant, the energy depends on displacement gradients, rather than the bare displacements. In addition, because it is rotationally invariant, the energy depends only on the symmetrization of these gradients, the small strains $\varepsilon_{ij} \equiv (\partial_i u_j + \partial_j u_i)/2$ [29,30]. The local energy then takes the general and well-known form $C_{ijkl}\varepsilon_{ij}\varepsilon_{kl}/2$, in terms of the three strain components $\varepsilon_{xx}, \varepsilon_{xy}, \varepsilon_{yy}$.

In contrast, consider an elastic structure containing a *mechanism*. In a coarse description, such a system is defined to contain a particular strain pathway that, as was the case with rotations, does not contribute to the elastic energy density. As shown in Supplemental Material [31], Sec. I. B, it is still always possible to construct orthonormal components of strain that separate this *mechanism strain* ε_m from the nonmechanism strains ε_1, ε_2, as shown in Fig. 1(c). Such variables inherently span all possible energy costly strains and we may write the elastic energy in general form as

$$E = \frac{1}{2}\int \mathrm{d}^2\mathbf{R}\,(G_{11}\varepsilon_1^2 + G_{22}\varepsilon_2^2 + 2G_{12}\varepsilon_1\varepsilon_2) \qquad (1)$$

in terms of these variables. The stiffnesses G_{ij} also define the constitutive relationship between the strains and the corresponding stresses, which is written compactly,

$$\begin{bmatrix}\sigma_m\\ \sigma_1\\ \sigma_2\end{bmatrix} = \begin{bmatrix}0 & 0 & 0\\ 0 & G_{11} & G_{12}\\ 0 & G_{12} & G_{22}\end{bmatrix}\begin{bmatrix}\varepsilon_m\\ \varepsilon_1\\ \varepsilon_2\end{bmatrix}, \qquad (2)$$

using the Voigt convention of treating stress and strain tensors as vectors of orthonormal components. Energy conservation requires the symmetry of this matrix, so that the presence of the mechanism eliminates three of the six independent stiffnesses. Thus, the defining property that the mechanism strain alone cannot generate stress also implies that mechanism stress with the same tensorial form cannot be supported $\sigma_m = 0$.

In the principal axis coordinates we choose, the mechanism strain tensor is diagonal and characterized solely by the mechanism Poisson's ratio ν, which is the negative ratio of strains along the axes. We note that a quarter-turn of the coordinate system inverts the Poisson ratio. Despite this ambiguity, the mechanism strain can only switch from auxetic ($\nu < 0$) to anauxetic ($\nu > 0$) by passing through the uniaxial strains where the Poisson's ratio either vanishes or diverges.

We investigate this general mechanism-based elasticity theory using the example structures displayed in Figs. 1(a) and 1(b), which are composed of rigid parallelograms connected at their corners by ideal frictionless hinges. Simultaneously rotating each block in opposite fashion to its neighbors does not cost any energy and this rotational motion therefore constitutes a mechanism. In addition to generating finely detailed rearrangements within each unit cell, this mechanism motion generates changes to the lattice vectors connecting each unit cell to its neighbors [Figs. 1(a) and 1(b), pink arrows]. The mechanism elasticity theory above then applies to a coarse description of the material deformation in terms of these lattice vectors. As shown in Fig. 1(d), varying the parallelogram angle ψ and mechanism rotation θ spans the possible values of the Poisson's ratio ν and, paired with a rotation of the coordinate system, any desired linear mechanism strain may be probed.

Sheared analytic modes.—For the special case of pure-dilational mechanisms, zero-energy deformations are those that disallow shear and hence preserve angles in the material. As is well-known, maps with this property are complex-analytic. That is, when points in the real plane are mapped to the complex plane, $(z, z^*) \equiv (x + iy, x - iy)$ with the equivalent map for displacements $(u, u^*) \equiv (u_x + iu_y, u_x - iu_y)$ (see, e.g., [33]), the zero-energy (i.e., stress-free) deformations are precisely those that satisfy *complex analyticity*, $\partial_{z^*} u = \partial_z u^* = 0$, which has yielded tremendous insight into dilational metamaterials [24–26].

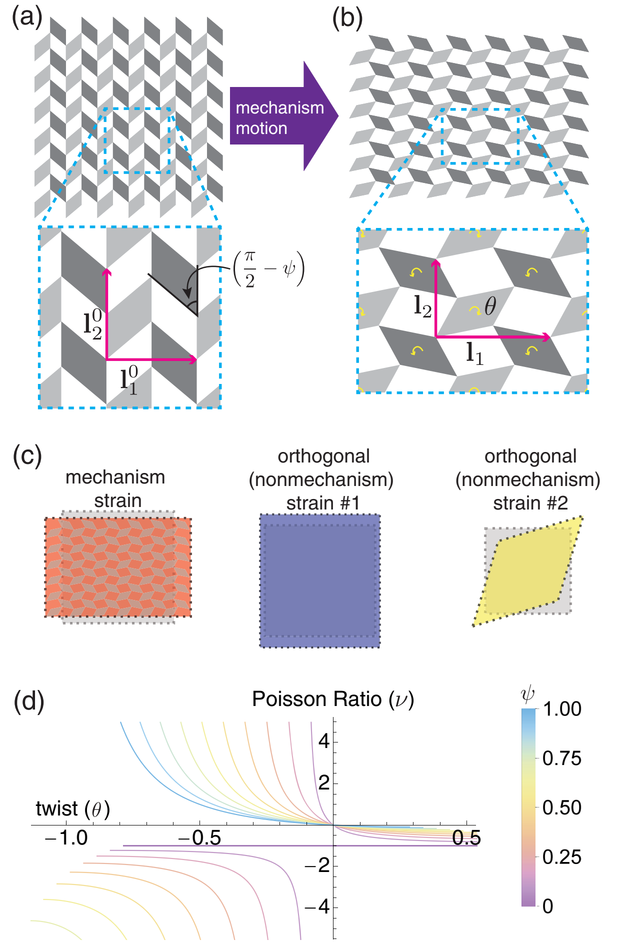

FIG. 1. A characteristic class of planar mechanisms. (a) The parallelogram-based mechanism designs we investigate are generated by setting a design angle ψ, and includes the canonical "Rotating Squares" pattern at the point $\psi = 0$. (b) The mechanism itself is traversed via rotating each rigid parallelogram (dark gray) opposite to its neighbors (light gray), which alters the macroscopic strain as reflected in the lattice vectors (pink arrows). Light and dark gray block coloration is purely for ease of viewing. (c) An appropriately chosen orthonormal basis may be used to decompose any arbitrary strain into mechanism and nonmechanism components as shown. (d) The strains generated by varying the counter-rotation θ for a variety of different ψ (different lines) capture an arbitrary variety of Poisson's ratios.

Thus motivated, we seek to extend this analyticity to generic mechanisms outside of the pure-dilational limit. This can be achieved by introducing the transformed variables:

$$\begin{bmatrix}w\\ \bar{w}\end{bmatrix} \equiv \begin{bmatrix}1 & \frac{1}{\gamma}\\ 1 & -\frac{1}{\gamma}\end{bmatrix}\begin{bmatrix}x\\ y\end{bmatrix}, \qquad (3)$$

$$\begin{bmatrix}u\\ \bar{u}\end{bmatrix} \equiv \begin{bmatrix}1 & -\gamma\\ 1 & \gamma\end{bmatrix}\begin{bmatrix}u_x\\ u_y\end{bmatrix}, \qquad (4)$$

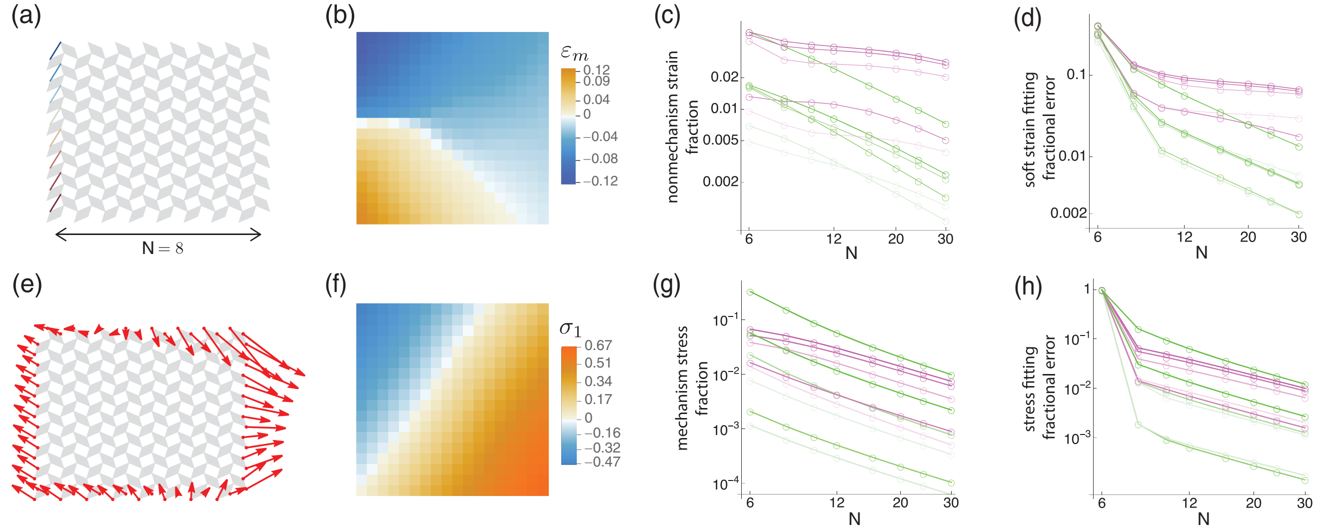

FIG. 2. Unimode mechanics in lattice metamaterials. (a)–(d) Minimal loading that is compatible with soft (stress-free) motions yields mechanism dominated soft strain patterns. (a) The systems deform due to a set of additional springs at the system left boundary that extend according to a smoothly varying function through space. (b) The mechanism strain ε_m exhibits significant variation through space. (c),(d) The fraction of strain orthogonal to the mechanism strain (the nonmechanism strain fraction) decreases, and the fitting to the global analytic form for soft strains improves as the lattice structure becomes finer. (e)–(h) More strict loading that is not compatible with a soft motion may still be deciphered using sheared analytic functions. (e) Data for "stress-bearing" loading is generated via numerical relaxation of the interior subject to displacement constraint of the boundary nodes, as detailed in Supplemental Material [31], Sec. III. B. (f) The resultant nonmechanism stress (Supplemental Material [31], Sec. III. C) is finite and varies through space. (g),(h) This nonmechanism stress dominates increasingly (i.e., the mechanism stress fraction decreases), and the fitting to a sheared analytic mode (captured in the fractional fitting error) improves as the continuum limit is approached just as with the soft strains.

where $\gamma \equiv \nu^{-1/2}$ is real for anauxetic mechanisms and imaginary for auxetic ones.

The utility of this transformation is seen in the identification of zero-energy deformations. As shown in Supplemental Material [31], Sec. II. A, it transforms the requirement that the two nonmechanism strains vanish into the requirement that two of the derivatives vanish:

$$\partial_{\bar{w}} u = 0 \quad \rightarrow \quad u = f_1(w) \tag{5}$$

$$\partial_{w} \bar{u} = 0 \quad \rightarrow \quad \bar{u} = f_2(\bar{w}). \tag{6}$$

Hence, for a continuum stress-free deformation, the transformed displacement fields are each analytic functions of just one of the transformed coordinates, consistent with Ref. [14].

In simply connected domains, these functions may then be generated by simple series expansions, e.g., $f_1(w) = \sum_{n=0}^{\infty} C_n w^n$. The requirement that u_x, u_y be real-valued enforces nontrivial restrictions on the functions f_1, f_2. On the auxetic side, where coordinates $w, \bar{w}$ are complex-valued, we require that $f_1(w), f_2(\bar{w})$ be complex conjugates of one another. For the anauxetic side, $w, \bar{w}$ are real-valued and we simply require that f_1, f_2 be real-valued functions. As this recipe for generating energy-free continuum unimode deformations relies on sheared analytic functions of a sheared coordinate system, we refer to them as "sheared analytic modes." The exact mathematics of the conformal soft maps from [25] is easily recovered in the limit $\nu \rightarrow -1$.

In addition to such stress-free displacements, there are patterns of stress that satisfy the bulk equilibrium condition $\partial_i \sigma_{ij} = 0$ [30]. Upon making a transformation similar to Eq. (4)

$$\begin{bmatrix} \sigma \\ \bar{\sigma} \end{bmatrix} \equiv \begin{bmatrix} \sqrt{2/(1+\nu^2)} & -\gamma \\ \sqrt{2/(1+\nu^2)} & \gamma \end{bmatrix} \begin{bmatrix} \sigma_1 \\ \sigma_2 \end{bmatrix}, \tag{7}$$

these conditions for force balance may be captured simply with

$$\partial_{\bar{w}} \sigma = 0 \quad \rightarrow \sigma = g_1'(w) \tag{8}$$

$$\partial_{w} \bar{\sigma} = 0 \quad \rightarrow \bar{\sigma} = g_2'(\bar{w}). \tag{9}$$

It is clear that this is again the same set of equations that were governing the stress-free displacement patterns. Beyond the immediate analytic insight this generates, Eqs. (8) and (9) indicates that the responses to "stress-free" (i.e., not requiring force) versus "stress-bearing" loading are mathematically dual spaces; any solution to one problem can readily be transformed into a solution to a dual problem in the other using a duality transformation T. Definitionally [34], this transformation, which here maps a

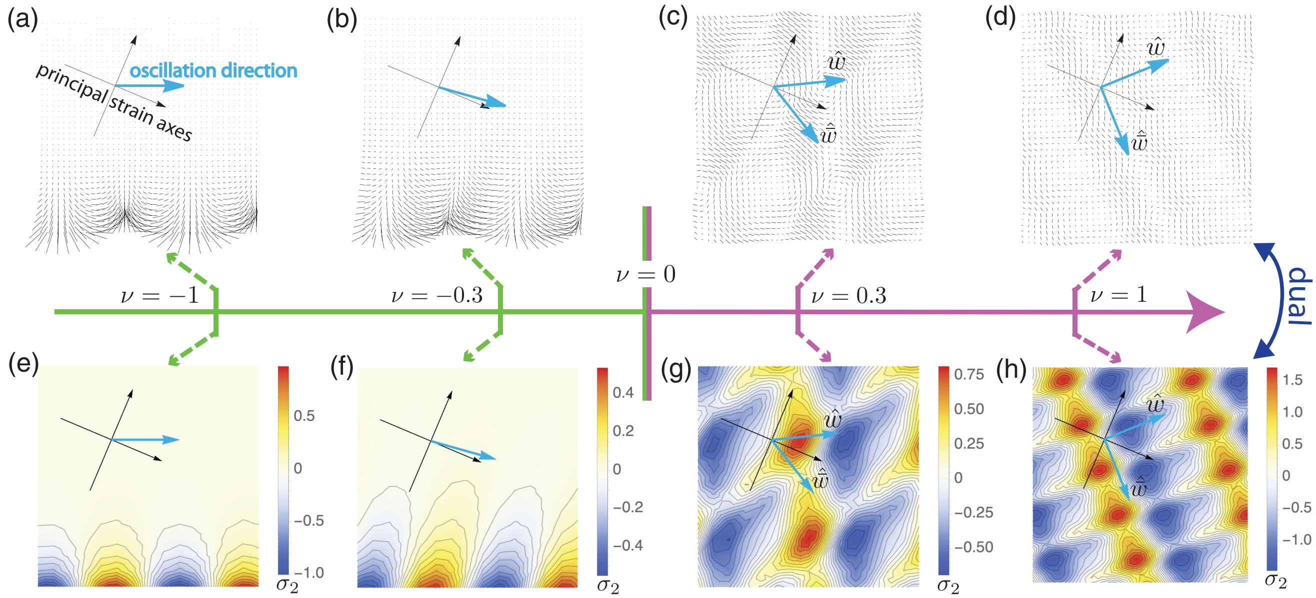

FIG. 3. Spatial distribution of static unimode response near an open boundary. (a)–(d) Stress-free continuum deformations of the unimode metamaterial in the semi-infinite plane, with arbitrarily oriented mechanism principal strain axes (large black arrows) will change character as an exceptional point is crossed at Poisson's ratio $\nu = 0$. For the auxetic systems in (a) and (b), an oscillatory set of displacements (black lines) along the open boundary (bottom edge) will decay into the bulk along the perpendicular, while oscillating in a special direction (blue arrow) set by the specific boundary orientation and by ν. (c),(d) On the other side of the exceptional point, the soft displacements of the anauxetic mechanism will oscillate into the bulk without decay, and as discussed in Supplemental Material, Sec. II. C [31] the boundary conditions on the transverse components may change with the addition of more modes when the longitudinal component is fixed. (e)–(h) The same unimode metamaterial, subjected to stressed boundary conditions, will display identical spatial patterns in the stress distribution due to the duality.

pattern of (dimensionless) soft displacement $s_1 = \{u, \bar{u}\}$ to a force-balanced stress $s_2 = (\sigma, \bar{\sigma}) = T(s_1)$, must constitute an involution, so that $s_1 = T(s_2)$. For the case here, this transformation is captured simply by the identity transformation, explored in greater depth using stress and strain fields in Supplemental Material [31], Sec. II. C.

To confirm these suggestive results, we examine numerically force-balanced states of our unimode material in both stress-free (Figs. 2(a)–2(d)) and stress-bearing (Figs. 2(e)–2(h)) load situations as the unit cell structure becomes finer. In both cases, following the analyses described in the S.I., our analytic framework captures the vast majority ($> 95\%$) of observed deformation and stress, and the quality of fit ubiquitously improves as the system size is increased. In other words, sheared analytic modes take hold and control response as the continuum limit of these materials is approached.

Spatial character of generic unimode response.—As a mechanism is tuned from the auxetic to the anauxetic, the sheared coordinate systems w and $\bar{w}$ briefly converge, becoming equal at $\nu = 0$ and then real for $\nu > 0$. This defines an exceptional point separating auxetic and anauxetic metamaterial mechanisms. Rather than controlling the more common energetic spectra [35] or phase transitions [36] for nonconservative systems, this is an exceptional point in a spatial coordinate transform, and thus distinguishes between spatial patterning types. On the auxetic side, the components of the displacement for a sheared analytic mode obey elliptic partial differential equations (see e.g., [37]) and are harmonic conjugate functions of the sheared coordinates. On the anauxetic side, these components remain conjugate, but as real-valued functions outside of the complex analytic setting; these components obey partial differential equations of hyperbolic character.

To illustrate these response patterns, we consider the infinite half-plane, of arbitrary orientation, and with the component of displacement along the boundary fixed to an oscillatory function. As shown in Figs. 3(a) and 3(b), the auxetic response decays into the bulk while simultaneously oscillating in a direction determined by both ν and orientation of the mechanism principal axes. As $\nu \to 0$ approaches the exceptional point from the negative side, the length scale of spatial decay diverges, eventually leading to persistent bulk oscillatory response in the anauxetic case.

This behavior may be exploited in a long strip geometry. Here, an arbitrary displacement input on one boundary may be decomposed into contributions of two polarization types, which rotate in opposite directions along the boundary. As derived in Supplemental Material, Sec. II. D and shown in Fig. 4, left-polarized components decay exponentially into the bulk of the auxetic metamaterial, while

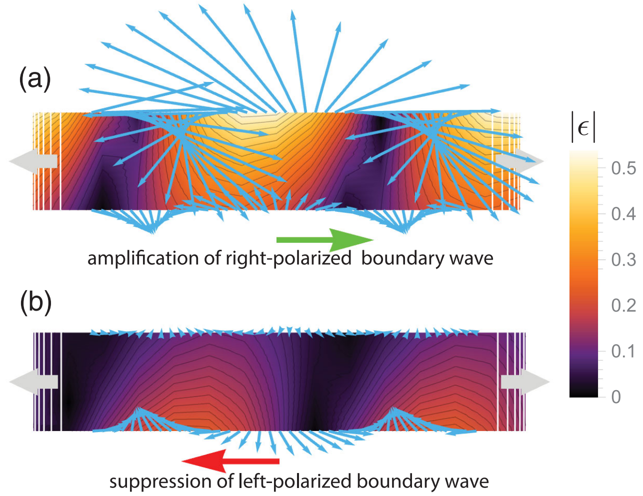

FIG. 4. Auxetic Unimode for Filtering of Mechanical Signals. (a) For an auxetic mechanism, a long strip of material will amplify incident displacement loads with polarization to the right. Polarization of input signal is the direction of travel in which the displacements would appear to rotate counterclockwise. (b) Shows the opposite exponential suppression of the opposite polarization input.

the right-polarized components will be amplified. As such, the unimode material acts not only as a mechanical amplifier but also as a filter that polarizes generic inputs, an initially generic static response. Note that, because of the duality, similar amplification and filtering will persist for stressed boundary conditions. Furthermore, as the structure traverses the mechanism motion, undergoing uniform large deformations, the Poisson's ratio itself changes sign, as shown in Fig. 1(d). This filtering property may therefore be switched on and off, with large applied strains acting as a "gating voltage" for mechanical signal processing in analogy with transistors.

Discussion.—We have shown that the presence of a single mechanism (unimode) in two-dimensional elasticity, as can be achieved in mechanical metamaterials, ubiquitously separates static response into dual spaces of stress-bearing and stress-free deformation that span all possible response patterns. Aside from an early indication of the role of analyticity [14], previous investigations have not addressed the stress-bearing response and have yielded partial, yet useful, insight into stress-free deformations by focusing only on unique (i.e., conformal) limits [24,25] and particular structural compositions [26,27]. In contrast, our investigation yields complete closed-form analytic results determined solely by the orientation and Poisson's ratio of the mechanism principal strain, thereby unifying response across structural designs and loading conditions. These results therefore apply to unimode structures composed of more varied combinations of polygons [5,24], realizing designer deformation pathways [38], achieving arbitrary range of deformation [39], and even those achieved via guided pruning algorithms on random networks [40]. The tunable Poisson's ratio ν, and particularly the exceptional point at $\nu = 0$, open the door to switchable elastic behavior, which we introduce, and which may become useful in metamaterial devices to amplify and filter signals in mechanical computing and circuitry [41].

The duality between the spatial patterns of stresses and strains joins an impressive contingent of dualities in mechanics, such as those of Maxwell and Cremona [42,43] between force balance and position compatibility, of the phonon dispersions of special dilational metamaterials [15], and that between elasticity and tensor gauge theories [44]. The duality presented herein appears to hinge on a type of mechanical criticality present in two-dimensional unimode metamaterials. Mechanism strain and rotation constitute two fields whose spatial variation must satisfy compatibility conditions, captured by a pair of first-order partial differential equations (Supplemental Material, Sec. I, and Refs. [25,26,28]). It is this balance of fields and partial differential equations that is crucial to our Letter and the two permitted stress fields likewise are constrained by two first-order partial differential equations that guarantee a force balance. It is an open question, then, how such general principles extend to three-dimensional flexible mechanical metamaterials, either bulk ones or curved two-dimensional surfaces [2,45–50].

We acknowledge helpful conversations with Corentin Coulais and Martin van Hecke.

[1] M. Kadic, T. Bückmann, N. Stenger, M. Thiel, and M. Wegener, Appl. Phys. Lett. **100**, 191901 (2012).
[2] K. Bertoldi, V. Vitelli, J. Christensen, and M. van Hecke, Nat. Rev. Mater. **2**, 17066 (2017).
[3] S. Li, H. Fang, S. Sadeghi, P. Bhovad, and K. W. Wang, Adv. Mater. **31**, 1805282 (2019).
[4] P. Dieleman, N. Vasmel, S. Waitukaitis, and M. van Hecke, Nat. Phys. **16**, 1 (2019).
[5] L. Liu, G. P. Choi, and L. Mahadevan, Proc. R. Soc. A **477**, 20210161 (2021).
[6] M. Meloni, J. Cai, Q. Zhang, D. S.-H. Lee, M. Li, R. Ma, T. E. Parashkevov, J. Feng, M. Meloni, J. Cai, Q. Zhang, R. Ma, J. Feng, D. S.-H. Lee, M. Li, and T. E. Parashkevov, Adv. Sci. **8**, 2000636 (2021).
[7] Z. G. Nicolaou and A. E. Motter, Nat. Mater. **11**, 608 (2012).
[8] T. Bückmann, M. Thiel, M. Kadic, R. Schittny, and M. Wegener, Nat. Commun. **5**, 1 (2014).
[9] C. L. Kane and T. C. Lubensky, Nat. Phys. **10**, 39 (2014).
[10] J. Paulose, A. S. Meeussen, and V. Vitelli, Proc. Natl. Acad. Sci. U.S.A. **112**, 7639 (2015).
[11] J. Paulose, B. G. G. Chen, and V. Vitelli, Nat. Phys. **11**, 153 (2015).
[12] K. K. Dudek, D. Attard, R. Caruana-Gauci, K. W. Wojciechowski, and J. N. Grima, Smart Mater. Struct. **25**, 025009 (2016).

[13] L. Wu, B. Li, and J. Zhou, ACS Appl. Mater. Interfaces **8**, 17721 (2016).
[14] D. Z. Rocklin, S. Zhou, K. Sun, and X. Mao, Nat. Commun. **8**, 1 (2017).
[15] M. Fruchart, Y. Zhou, and V. Vitelli, Nature (London) **577**, 636 (2020).
[16] A. Bossart, D. M. Dykstra, J. van der Laan, and C. Coulais, Proc. Natl. Acad. Sci. U.S.A. **118**, e2018610118 (2021).
[17] C. Scheibner, A. Souslov, D. Banerjee, P. Surówka, W. T. Irvine, and V. Vitelli, Nat. Phys. **16**, 475 (2020).
[18] L. Jin, R. Khajehtourian, J. Mueller, A. Rafsanjani, V. Tournat, K. Bertoldi, and D. M. Kochmann, Proc. Natl. Acad. Sci. U.S.A. **117**, 2319 (2020).
[19] S. H. Kang, S. Shan, A. Kosmrlj, W. L. Noorduin, S. Shian, J. C. Weaver, D. R. Clarke, and K. Bertoldi, Phys. Rev. Lett. **112**, 098701 (2014).
[20] S. Armon, H. Aharoni, M. Moshe, and E. Sharon, Soft Matter **10**, 2733 (2014).
[21] R. Gatt, L. Mizzi, J. I. Azzopardi, K. M. Azzopardi, D. Attard, A. Casha, J. Briffa, and J. N. Grima, Sci. Rep. **5**, 1 (2015).
[22] C. Coulais, A. Sabbadini, F. Vink, and M. van Hecke, Nature (London) **561**, 512 (2018).
[23] J. A. Michel and P. J. Yunker, Proc. Natl. Acad. Sci. U.S.A. **116**, 2875 (2019).
[24] K. Sun, A. Souslov, X. Mao, and T. C. Lubensky, Proc. Natl. Acad. Sci. U.S.A. **109**, 12369 (2012).
[25] M. Czajkowski, C. Coulais, M. van Hecke, and D. Z. Rocklin, Nat. Commun. **13**, 1 (2022).
[26] Y. Zheng, I. Niloy, P. Celli, I. Tobasco, and P. Plucinsky, Phys. Rev. Lett. **128**, 208003 (2022).
[27] Y. Zheng, I. Tobasco, P. Celli, and P. Plucinsky, Proc. R. Soc. A **479**, 20220665 (2023).
[28] M. Czajkowski and Z. Rocklin, Bull. Am. Phys. Soc. B17 (2021).
[29] P. Chaikin and T. Lubensky, *Principles of Condensed Matter Physics* (Cambridge University Press, Cambridge, England, 2000).
[30] L. Landau, E. Lifšic, E. Lifshitz, A. Kosevich, J. Sykes, L. Pitaevskii, and W. Reid, *Theory of Elasticity: Volume 7*, Course of Theoretical Physics (Elsevier Science, New York, 1986).
[31] See Supplemental Material at http://link.aps.org/supplemental/10.1103/PhysRevLett.132.068201 for a more in-depth discussion of this duality, which includes Refs. [32].
[32] G. K. Batchelor, J. Fluid Mech. **41**, 545 (1970).
[33] A. England, *Complex Variable Methods in Elasticity*, Dover Books on Mathematics Series (Dover Publications, New York, 2003).
[34] M. Fruchart and V. Vitelli, Phys. Rev. Lett. **124**, 248001 (2020).
[35] M.-A. Miri and A. Alú, Science **363**, eaar7709 (2019).
[36] M. Fruchart, R. Hanai, P. B. Littlewood, and V. Vitelli, Nature (London) **592**, 363 (2021).
[37] M. Stone and P. Goldbart, *Mathematics for Physics: A Guided Tour for Graduate Students* (Cambridge University Press, Cambridge, England, 2009).
[38] G. P. T. Choi, L. H. Dudte, and L. Mahadevan, Nat. Mater. **18**, 999 (2019).
[39] G. W. Milton, J. Mech. Phys. Solids **61**, 1543 (2013).
[40] C. P. Goodrich, A. J. Liu, and S. R. Nagel, Phys. Rev. Lett. **114**, 225501 (2015).
[41] H. Yasuda, P. R. Buskohl, A. Gillman, T. D. Murphey, S. Stepney, R. A. Vaia, and J. R. Raney, Nature (London) **598**, 39 (2021).
[42] W. F. Baker, L. L. Beghini, A. Mazurek, J. Carrion, and A. Beghini, Struct. Multidiscip. Optim. **48**, 267 (2013).
[43] R. P. Behringer and B. Chakraborty, Rep. Prog. Phys. **82**, 012601 (2018).
[44] M. Pretko and L. Radzihovsky, Phys. Rev. Lett. **120**, 195301 (2018).
[45] M. Schenk and S. D. Guest, Proc. Natl. Acad. Sci. U.S.A. **110**, 3276 (2013).
[46] H. Aharoni, E. Sharon, and R. Kupferman, Phys. Rev. Lett. **113**, 257801 (2014).
[47] H. Nassar, A. Lebée, and L. Monasse, Proc. R. Soc. A **473**, 20160705 (2017).
[48] H. Nassar, A. Lebée, and E. Werner, Extreme Mech. Lett. **53**, 101722 (2022).
[49] J. T. B. Overvelde, J. C. Weaver, C. Hoberman, and K. Bertoldi, Nature (London) **541**, 347 (2017).
[50] I. Griniasty, H. Aharoni, and E. Efrati, Phys. Rev. Lett. **123**, 127801 (2019).